A SURVEY OF THE BACKGROUND RADIATION AT A FREQUENCY OF 404 Mc/s

I. I. K. Pauliny-Toth and J. R. Shakeshaft

(Received 1961 December 22)

Summary

This paper describes measurements of the brightness temperature of the sky as measured at 404 Mc/s with a beam of width 7°·5 between half-power points. The region surveyed lies between declinations −20° to +90°. The observed noise powers have been compared with those available from resistances at different temperatures and particular attention has been paid to corrections for radiation received in side-lobes of the beam from the ground and other parts of the sky. The average error in the brightness temperature differences between any two points observed is believed to be ±0·8 °K and the error in the absolute temperature at an average point is about ±2·2 °K.

---

1. *Introduction.*—In order to test theories of the radio emission from the Galaxy, it is important to determine the variation of the intensity of the emission with frequency. The aim of the present observations has been to derive a map of the sky brightness at 404 Mc/s which may be compared with maps at lower frequencies to obtain the spectral law for the emission from each different region of the Galaxy. Such maps (**1, 2, 3**) have recently been made at the Mullard Radio Astronomy Observatory by using similar observational methods to those employed in the present survey.

The difficulties of achieving a given accuracy in such observations increase with increasing frequency, for the brightness temperature of the sky decreases rapidly so that corrections for radiation from the ground and losses in the aerial system become relatively more important. A frequency of 404 Mc/s was chosen as being in a band "free" from interference, sufficiently far removed in frequency from the surveys mentioned above to provide useful spectral information and yet not so high that the problems involved would become too formidable.

The survey was made with an aerial of comparatively small resolving power, the beamwidth being about 7°·5 between half-power points, but one which allowed accurate corrections to be made for ground radiation. Surveys of greater resolution have been made at this frequency (**4, 5**) but it is believed that the present observations provide a more accurate representation of the large scale features of the radiation and that the scale of brightness temperature and the zero level are defined more closely.

The accurate measurement of the sky brightness temperature in the main beam of the reception pattern requires: (i) absolute measurements of available noise power; (ii) a correction for losses in the aerial and connecting cables; and

(iii) a knowledge of the reception pattern of the aerial over all angles and the contribution to the power received by radiation from other parts of the sky and from the ground. Details of the methods used are given in this paper.

The observations were made between 1960 September and 1961 March and consisted of two separate programmes: (i) the main survey in which the brightness temperatures of a grid of points across the sky were compared with that at the North Celestial Pole; and (ii) the measurement of the brightness temperature of the North Celestial Pole.

2. *The apparatus*

(i) *The aerial system.*—The aerial was a 7·5 m paraboloid with a focal ratio of 0·23, on an alt-azimuth mount. A simple dipole and reflector feed was fixed at the focus, with the dipole horizontal. The beamwidth of the aerial was 8°·5 in the E-plane and 6°·5 in the H-plane and the forward gain, determined from reception pattern measurements, was 27·4 db. The feed was supported by an air-spaced brass coaxial line, 2 m long and of 72 ohms impedance, which led along the axis of the dish to its apex and formed a low-loss assembly with the dipole. A flexible coaxial cable connected the lower end of the air-spaced line to the switch and receiver, which were housed in a hut on the telescope platform. By adjustment of the length of the dipole and of the spacing between the dipole and the reflector, the standing wave ratio on the coaxial line was reduced below 0·5 db.

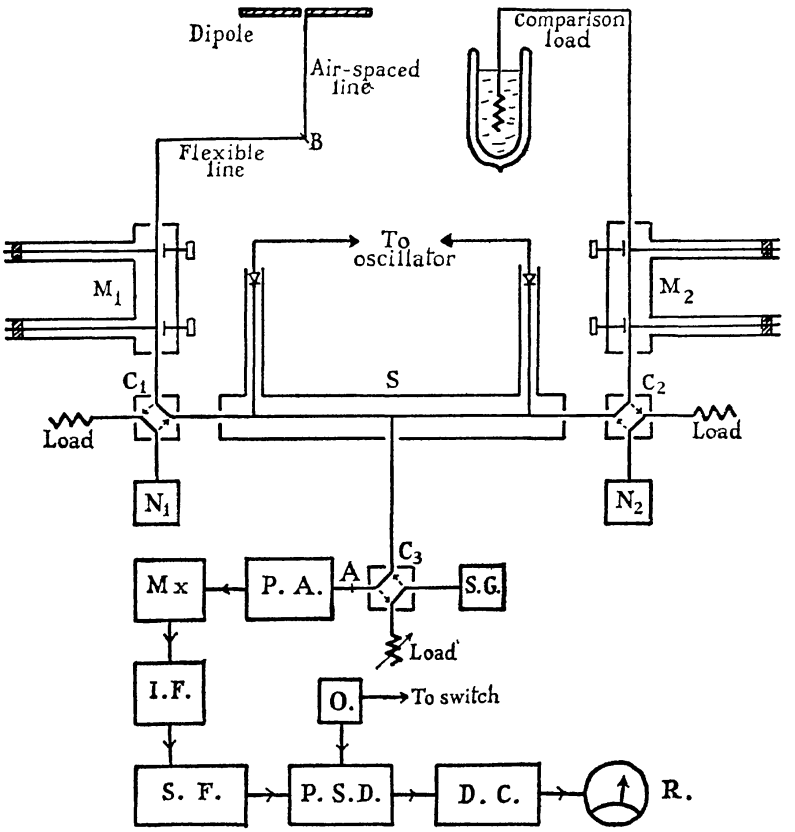

FIG. 1.—*The receiving system.* S.G., *signal generator*; P.A., *parametric amplifier*; Mx, *mixer*; I.F., *intermediate frequency amp. and detector*; S.F., *switch frequency amp.*; P.S.D., *phase-sensitive detector*; D.C., *d.c. amplifier*; R., *pen recorder*; O., *square wave oscillator.*

(ii) *The receiver.*—The receiving system was of the Dicke type (**6**) in which the noise power available from the aerial was compared with that from a resistance of the same impedance maintained at the temperature of liquid nitrogen. The comparison was achieved by switching the receiver input between the aerial and the resistive load at 270 c.p.s. The switch, illustrated schematically in Fig. 1, was constructed of air-spaced coaxial line. It had two 1N 270 diodes at the end of $\lambda/4$ stubs, $\lambda/2$ apart, with the output taken from the mid-point of the $\lambda/2$ line. The loss in the switch was 0·2 db.

The first stage of the receiver was an electron beam parametric amplifier, of the Adler type, operating in the degenerate mode, that is with the pump frequency at 808 Mc/s. The gain of the amplifier was 24 db and the excess input noise temperature was 130 °K. The stability of the gain was good and any small changes that occurred were eliminated by automatic gain control in the main receiver. The subsequent mixer, intermediate frequency amplifier, switch-frequency amplifier and synchronous detector followed standard practice. A 2 Mc/s filter was included in the intermediate frequency amplifier for reasons discussed later. A block diagram of the complete receiving system is shown in Fig. 1.

The system noise was produced by the following sources:

(*a*) on the aerial side of the switch the average sky contribution was about 30 °K, with losses in the feed system giving 6 °K and in the connecting cable 30 °K, a total noise of 66 °K;

(*b*) on the load side of the switch, the noise from the comparison load and connecting cable was 82 °K;

(*c*) losses in the switch assembly gave some 25 °K;

(*d*) the input noise of the parametric amplifier was 130 °K;

(*e*) the second stage contributed about 10 °K.

The total system noise was therefore about $165+\frac{1}{2}(66+82)$ or 239 °K. With a bandwidth of 2 Mc/s and a time constant of 4 sec the expected r.m.s. fluctuations on the output are $\pm 0{\cdot}15$ °K; those observed were $\pm 0{\cdot}2$ °K.

(iii) *The comparison load.*—The comparison load consisted of a carbon film resistor, terminating a half-wavelength of coaxial line which was made of German silver to reduce heat conduction. The resistance itself was in direct contact with the liquid nitrogen, the outer conductor of the line being extended as a wire cage (Fig. 2).

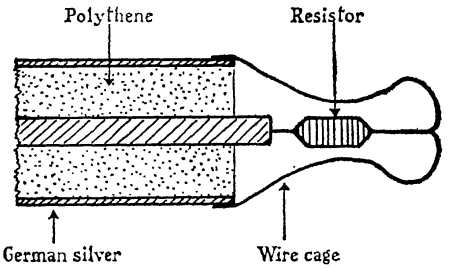

FIG. 2.—*The comparison load.*

The space between the inner and outer conductors was filled with polythene to prevent liquid nitrogen from entering the line and causing changes of impedance

as the nitrogen level altered. Despite this precaution, small changes of impedance were still detectable as the nitrogen level changed, but these were corrected by the methods described below.

By a suitable choice of resistor and by adjusting the shape of the wire cage, the impedance of the load in liquid nitrogen was made entirely resistive, differing from the characteristic impedance of the coaxial lines used (72 ohms) by less than 5 per cent. The resistor was kept immersed at least six inches below the surface of the nitrogen in a thermos flask. Its temperature was therefore equal to that of the liquid nitrogen, which was taken to be 77·3 °K. A small orifice allowed nitrogen gas to escape without permitting air to enter the thermos flask and condense in the liquid nitrogen, thus changing its boiling-point. Variations of the boiling-point with pressure are small and were neglected. The deviations of the temperature of the liquid nitrogen from 77·3 °K could not have been more than +0·5 °K, corresponding to changes of barometric pressure of 25 mm of mercury or a proportion of dissolved oxygen of 5 per cent. Including a correction for the loss of the German silver coaxial line, the effective temperature of the reference load was 77·5 °K.

(iv) *The impedance matching networks.*—In general, the output from an amplifier depends on the impedance of the input load, and the electron beam parametric amplifier is no exception to this rule. The change of output may be attributed to the reflection back on to the beam of the noise power stripped off the beam by the input coupler. With the tube used in these observations the original beam fluctuations correspond to a noise temperature of some 800 °K. The effect of an input mismatch is twofold: first, it reduces the sensitivity by increasing the system noise; secondly, and much more important, it produces a signal at the switching frequency unless the impedance of the aerial and comparison load are identical. If the zero level on the record is to be kept constant to within ±0·1 °K of aerial temperature, the impedances must be maintained equal to within 1 or 2 per cent. It was found that condensation of moisture on the dipole, flexure of the coaxial cable between the aerial and the switch, and changes in impedance of the comparison load could produce significant zero displacements; a system was therefore employed which allowed the impedances of both the aerial and the comparison load to be measured and adjusted both easily and rapidly. It has been described briefly in a paper by Smith (**7**).

The system is shown in Fig. 1. The signals from the aerial and the load both passed through matching units (M_1, M_2) then through directional couplers (C_1, C_2) to the crystal switch (S). The directional couplers were similar to those described by Monteath (**8**). They were designed to have a coupling of −20 db and were used in conjunction with the noise sources N_1, N_2 in the calibration of the sensitivity of the system.

The matching units consisted of two shorted stubs, $\lambda/8$ apart, on an air spaced coaxial line. The stub-lengths were set up at the start of the observations and small capacitance variations were thereafter provided by micrometer screws projecting into the coaxial line. The output of the switch was connected through a third directional coupler (C_3) to the input of the parametric amplifier.

The initial setting-up procedure involved the application of d.c. potentials to the switch diodes so that the aerial, for example, was connected. The impedance of the aerial itself was already close to 72 ohms but by use of the fine controls on M_1, the impedance at point A was adjusted to a matched condition

as observed with a slotted line. A C.W. signal at 404 Mc/s was then injected into arm 1 of the coupler C_3, arm 2 being terminated in a variable impedance. In such a case a corresponding signal is induced travelling towards the receiver. If the aerial impedance bears some fixed relationship to the impedance on arm 2, no net signal is detected by the receiver. M_1 having been adjusted to match the aerial, the variable impedance on arm 2 was adjusted so that no signal reached the receiver, and the impedance was left fixed at this value throughout the observations. Thereafter, whenever a C.W. signal was fed into arm 1 and the matching unit M_1 was adjusted to give no signal at the receiver, it was known that the aerial was precisely matched. The same procedure was used to adjust M_2, so that the impedances of the aerial and reference load were matched and equal. The impedances could be adjusted with an accuracy at least ten times greater than the 1 per cent required to reduce zero drifts to less than 0·1 °K. The whole matching procedure could be carried out in less than 30 seconds.

3. *The method of calibration.*—For convenience the noise power received from the aerial during observations was measured in terms of the anode current through a CV 2171 diode noise source (N_1) which could supply noise power to the aerial side of the switch through the directional coupler C_1. During observations the amount of noise supplied through this coupler was adjusted to bring the total noise power in the two switch positions to nearly the same value, and the output of the receiver was used merely as an incremental reading. By this means possible errors due to the non-linearity of the receiver were eliminated. For observations near the galactic plane, noise could also be supplied to the load side of the switch to make the noise powers equal.

The relation between the anode current of the noise source and the power available from a matched resistor was established in a subsidiary experiment, in which resistive loads at the temperature of liquid nitrogen, an ice-water mixture, and hot water at a known temperature were substituted for the aerial. The substitution was made at the point B (Fig. 1) and the matching procedure was carried out for each temperature. In each case, the anode current of the source N_1 required to produce the same receiver output was determined, giving the required relationship.

An absolute measurement of the noise power available from the aerial when this was directed at the North Celestial Pole was made by substituting a resistive load in liquid nitrogen for the aerial at the point B. The difference in noise power from the aerial and the load was found in terms of the calibrated noise source N_1. There are, however, two possible sources of error in this measurement. First, if the impedances of the aerial and the comparison load are adjusted to be equal by means of a C.W. signal at 404 Mc/s, they may not be equal over the whole bandwidth of the receiver, which will then receive a spurious signal at the switching frequency. Secondly, if the impedances of the substituted load and the aerial are not closely the same, the adjustment of the matching unit M_1 will produce a standing wave in the coaxial line between the load and the matching unit and therefore lead to an increase in the effective temperature of the load.

To eliminate the first effect, I.F. filters were used to give bandwidths of 4 Mc/s and 2 Mc/s at 500 kc/s. The matching adjustments were made for each bandwidth with a C.W. generator at the centre frequency and also with a noise source. It was found that for a bandwidth of 2 Mc/s or less, the same results were obtained with a noise source and a C.W. signal. Since a C.W.

signal generator was more convenient for day-to-day use, C.W. matching and a 2 Mc/s bandwidth were subsequently used.

To eliminate the second effect, the loads used were constructed to have an impedance close enough to that of the aerial for the contribution to the aerial noise power due to the standing wave to be negligible.

4. *Contributions to the aerial noise power*

(i) *General considerations.*—The quantity measured in the observations was the noise power available from the aerial (at point B in Fig. 1) as a function of the position of the beam in the sky. This measured power corresponds to a temperature T_e which is related to the temperature T_i of a loss-free aerial by the expression:

$$T_e=(1-\alpha)T_i+\alpha T_f$$

where α is the loss factor of the feed and the coaxial line to the point B, and T_f is the temperature of these components.

The temperature T_i may conveniently be divided into four parts:

$$T_i=T_m+T_s+T_g+T_0$$

where T_m is the contribution from the region of the sky within the main beam, T_s is the contribution from other regions of the sky radiating into side-lobes of the aerial, T_g originates from the ground, and T_0 is due to atmospheric attenuation.

It will be seen later that the atmospheric attenuation is small and that no appreciable error is introduced by neglecting the corrections for such attenuation which should strictly be applied to T_m and T_s before relating them to the actual brightness temperature of the sky.

The aim of the work was, in the first instance, to obtain absolute values of T_m+T_s, the part of T_i originating from the sky; then to derive T_m by calculating T_s, and finally to derive the "beam temperatures" T_b of the loss-free aerial with all its power in the main beam. If the proportion of power in the main beam is x, then

$$T_b=T_m/x=\frac{T_i-T_s-(T_g+T_0)}{x}.$$

The subtraction of (T_g+T_0) from the temperatures T_i may be carried out to a first order by observing a region of sky at different elevations. A curve is obtained showing how T_i for this region varies with elevation (Fig. 4). Suppose that T_i for this particular region changes by an amount ΔT_i between the zenith and another elevation. On the assumption that this change is the same for all regions of the sky, ΔT_i is subtracted from all observations made at this elevation to give the temperatures T_i which would be obtained if the observations had been made at the zenith. Subtraction of any ground and atmospheric contribution remaining at the zenith then gives a close approximation to T_m+T_s. We shall denote this approximation by T_a' and the exact value of T_m+T_s by the aerial temperature

$$T_a=T_i-(T_g+T_0)=T_m+T_s.$$

T_a is the effective temperature of a loss-free aerial, in a loss-free atmosphere, above a ground of zero brightness. The quantity given in Table 1 and plotted in the contour maps is T_a', since this is derived from the experimental data with a minimum of correction.

The difference between T_a' and T_a is due to the assumption that the curve of the change in T_i against elevation is due simply to variations of the ground contribution T_g and the atmospheric contribution T_0 with elevation. In fact, as the elevation of the region of sky observed in this experiment increases, not only does $T_g + T_0$ decrease but T_s increases, since the proportion of sky to ground in the side-lobes increases. The solid curve of Fig. 4 thus represents a difference between the decrease in $T_g + T_0$ and the increase in T_s with increasing elevation for the particular region of sky used to obtain the curve. It is shown later that the temperatures T_a' given in Table I are higher than the temperatures T_a defined earlier by an amount varying from zero at the zenith to 1 °K at declination $-20°$.

(ii) *The loss-factor of the feed.*—The loss-factor of the air-spaced coaxial line leading from the apex of the dish to the dipole was calculated to be 2·0 per cent. This loss-factor was also measured by short-circuiting the ends of the line in turn, and measuring the standing wave ratios on a slotted line connected to point B (Fig. 1). The measurement gave a value of $(2{\cdot}0 \pm 0{\cdot}2)$ per cent for the loss. The loss-factor of the dipole itself was calculated to be 0·2 per cent by treating it as a length of transmission line. The factor α of Section 4(i) was thus $(2{\cdot}2 \pm 0{\cdot}2)$ per cent. All observed noise powers could now be converted into the corresponding temperatures T_i.

(iii) *The aerial reception pattern.*—The response of the aerial system to radiation off the axis was investigated, using as a source first the Sun and secondly a transmitting dipole mounted close to the ground some 250 m from the dish.

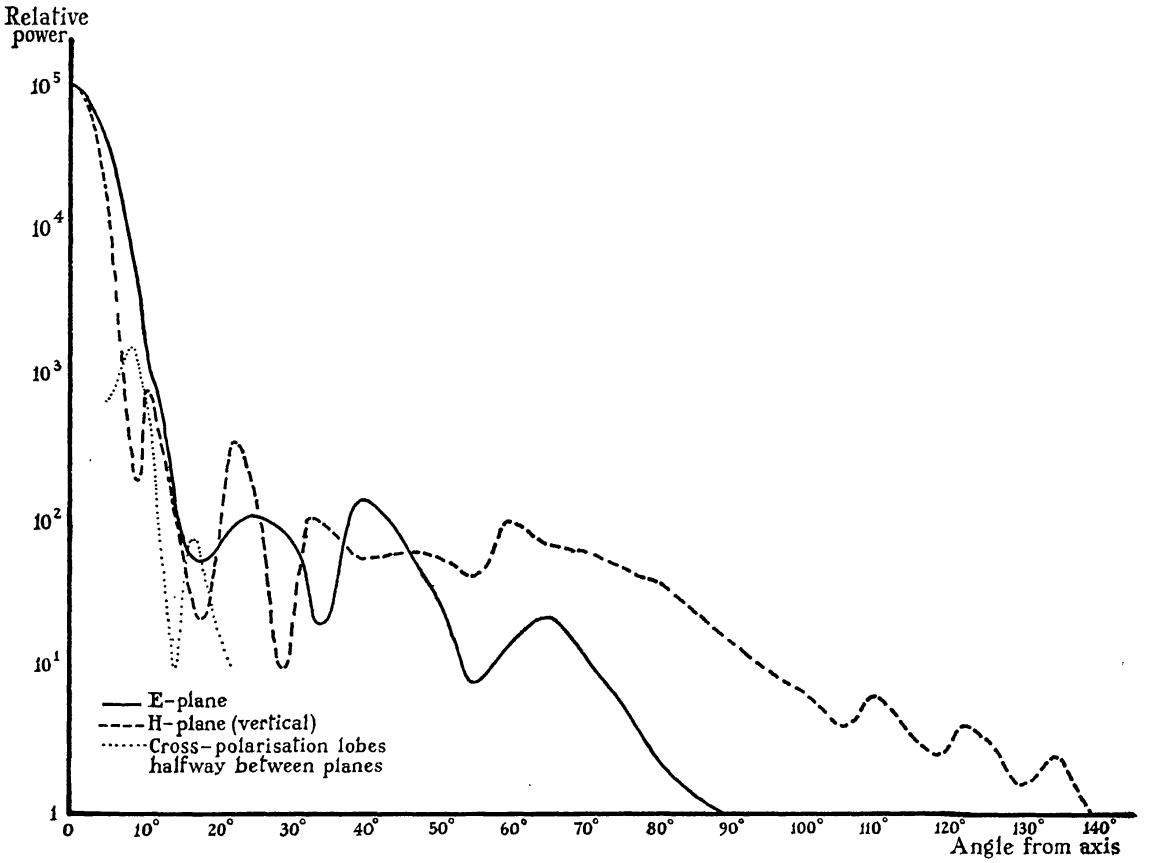

FIG. 3.—*The reception pattern of the aerial.*

The side-lobes produced by the Sun could be measured with sufficient accuracy up to 50° from the axis. For angles greater than this, the transmitter on the ground was relied on to obtain the side-lobe levels, and the zero level of the far-out pattern was determined by fitting it to the near-in pattern obtained from the Sun where the two overlapped. It was hoped in this way to reduce the errors produced by reflections from surrounding objects in the pattern obtained by using the transmitter. Measurements near the main beam were also made of the cross-polarization lobes in planes halfway between the principal planes. The patterns obtained are shown in Fig. 3.

Assuming that the pattern at a given angle off the axis varies smoothly between the values in the principal planes, calculation shows that the proportion of the power radiated by the aerial into the main beam (defined as a cone of semi-angle 10°) is 85 per cent, that 14 per cent of the power is radiated into the other forward lobes and less than 1 per cent into the back lobes. The other quantities which may be calculated for the aerial are:

the forward gain $= 27{\cdot}4$ db;
the effective area $= 24{\cdot}3$ m^2;
the area efficiency $= 55$ per cent.

(iv) *The atmospheric contribution* T_0.—Hogg (**9**) has evaluated this temperature as a function of frequency and elevation. His curves show that at 404 Mc/s and at elevations greater than 18° (corresponding to declination $-20°$ in this survey) the atmospheric contribution T_0 is less than 3 °K, that is, the loss factor of the atmosphere is less than 1 per cent. To the accuracy of the experiment, the attenuation may be treated as contributing a term T_0 to T_i, without affecting T_m and T_s. The change in T_0 with elevation is obtained in the experiment described below; the value of T_0 at the zenith is taken as 1 °K. The attenuation is mainly due to absorption by oxygen; it will not therefore vary appreciably with weather conditions.

(v) *The ground contribution* T_g.—It is not possible to measure this quantity alone nor to measure it absolutely. An approximation to $(T_g + T_0)$ was, however, obtained as follows. The changes in the aerial noise power (T_e) of several regions of sky near $\alpha\, 09^h$, at $\delta + 52°$, were observed while they were tracked from lower to upper culmination. These regions were chosen because at the latitude of the Observatory they pass through the zenith. The solid curve of Fig. 4 was thus obtained, showing the changes ΔT_i for these regions against elevation. This curve could be used to derive the temperature T_a' of any region of sky when the zero level of the curve was fixed as described below. The assumption is made, in correcting for ground radiation, that this is independent of azimuth. This assumption is justified by the similarity of the surroundings at different azimuths except at the lowest elevations, where the main beam intersects the ground. At the elevation of 18°, the error due to this assumption is thought to be less than 0·5 °K.

A calculation of the ground contributions was also made, using the measured reception pattern and assuming a ground brightness temperature of 250 °K in the vicinity of the aerial, which was surrounded by grass-covered earth-banks, and a ground brightness temperature of 125 °K for the distant ground which is observed at almost grazing incidence. The latter figure was deduced from a measurement of the aerial noise power at zero elevation. The atmospheric

contributions T_0 were obtained from Hogg's curves and added to the calculated values of T_g to give the points denoted by squares in Fig. 4.

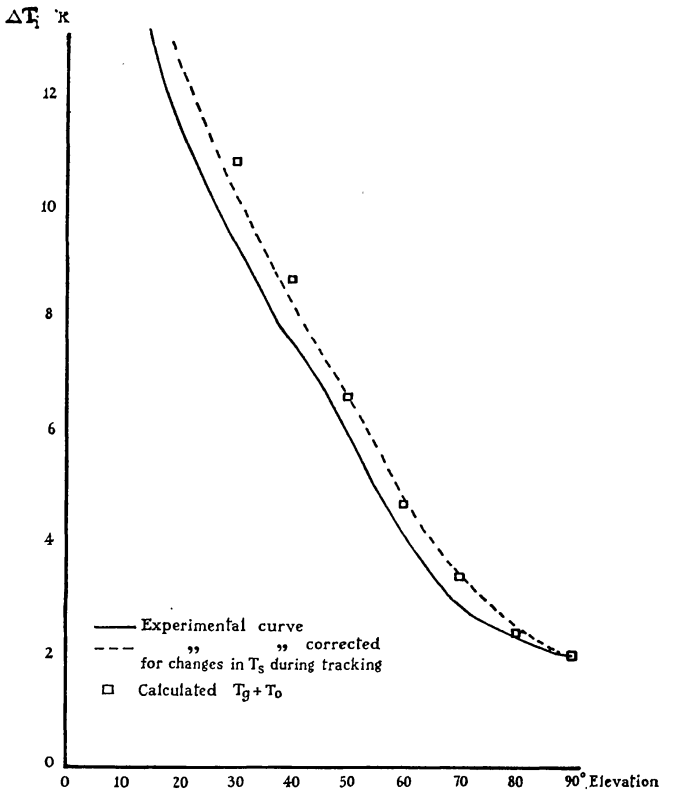

FIG. 4.—*The contribution of ground and atmospheric radiation.*

This calculation provides the absolute level of $(T_g + T_0)$ which is not obtained in the tracking experiment. It shows that when the aerial is directed towards the zenith, the radiation from the ground contributes about 1 °K to the aerial temperature, mostly from the zone between 90° and 120° off-axis. An experiment in which a reflecting screen 30 m square was placed under the dish and on the surrounding earth-banks produced no detectable decrease in T_i for regions of sky at the zenith, showing that radiation from the area covered was certainly less than 0·5 °K. The ground radiation at the zenith, then, originates from the area not covered by the screen, corresponding to angles from the dish axis of 90° to 110°, and an absolute level of radiation of about 1 °K. The atmospheric contribution at the zenith, as mentioned earlier, is about 1 °K. The zero of the curves in Fig. 4 was thus fixed at 2 °K.

It was explained in Section 4 (i) that the experimental curve is in error by a small amount owing to changes in T_s during the tracking. These changes may be computed as described below and the resulting curve, which represents the true values of $(T_g + T_0)$, is also given in Fig. 4 (broken curve).

(vi) *The sky contribution* T_s.—It is possible, by a process of successive approximations, to remove the effect of side-lobes outside the main beam. The temperatures T_a' were plotted on a sphere, and a grid representing the aerial reception pattern was superimposed on the sphere. The contributions T_s of regions of the sky outside the main beam were calculated with the pattern centred on

different points of the sky. A table of these contributions (Table II) was thus drawn up.

By the same method, the changes in T_s for the particular regions observed during the tracking experiment described above were calculated at successive elevations of the aerial. A table of corrections to the temperatures T_a' of Table I was obtained; when the corrections are subtracted, the temperatures T_a, as defined in Section 4 (i), are obtained. These corrections are:

Declination	−20°	−10°	10°	30°	52°	70°
Correction (°K)	1·1	0·9	0·7	0·5	0	0·4

Subtraction of the contributions T_s from T_a gives T_m, which may be thought of as the effective temperature of the aerial at the given point when all regions outside the main beam have zero brightness. The 'beam temperature' T_b is given by

$$T_b = (T_a - T_s)/0{\cdot}85$$

since 85 per cent of the power is in the main beam of the aerial. The differences between T_b, T_a and T_a' are generally small. For example, at $\delta + 10°$:

α(h)	0	4	8	12	16	19	22
T_a'	25·5	25·0	19·9	22·0	42·5	131	27·5
T_a	24·8	24·3	19·2	21·3	41·8	130	26·8
T_s	3·6	3·6	3·1	2·8	4·7	5·6	4·1
T_b	24·9	24·4	18·9	21·5	43·6	146	26·7

Only in the region of the galactic plane is there a significant difference between T_a' and T_b. In deriving the values of T_s the use of the T_a' distribution rather than the T_b distribution, which would have been more correct, was therefore justifiable.

In a comparison of different surveys, the corrections for the power in the side-lobes are of great importance. The reception patterns of both aerials must be known and the beam temperatures should be compared making allowance for any difference in the size of the beams. A comparison of the present survey with lower frequency surveys carried out at this observatory is described elsewhere (**10**).

5. *The determination of sky brightness temperatures relative to the pole.*—A grid of points spaced by 10° in declination and about 10° to 15° in right ascension was observed, with most of the observations being made at transit. The procedure during any night of observations was as follows. With the aerial directed at the North Celestial Pole, the sensitivity of the system was determined by feeding noise from the calibrated noise source N_1 into the directional coupler C_1. The aerial was then directed at the various declinations in turn. The matching of the dipole and comparison load was checked frequently and if necessary corrected. These checks prevented the zero level drifts mentioned in Section 2 (iv). After three or four points on the grid had been observed, the beam was again directed at the Pole for a few minutes, after which further points were observed. The noise source was calibrated at intervals throughout the survey and showed no change in its output greater than 1 per cent over the whole period. The noise power differences observed were corrected for the loss factor α and the experimental ground radiation curve (Fig. 4, solid line) was used to

change the observed differences between the points in the sky and the North Pole into those differences which would be observed if the points and the Pole were at the zenith.

Three surveys were made, between 1960 September and 1961 March, covering declinations $-20°$ to $+80°$ at 10° intervals, at right ascensions ranging from 20^h to 06^h, 05^h to 17^h and 16^h to 21^h. Observations were carried out at night as radiation from the Sun interfered with experiments in daytime. To make observations at night possible before March, the last of the three surveys was carried out $2\frac{1}{2}$ hours before the transit of the region across the meridian. The agreement in the regions of overlap of the three surveys was generally better than 0·5 °K, except in the last survey where dicrepancies of up to 1·5 °K occurred on some declinations. These could be explained by the effect of far-out side-lobes, since in the last survey the sky was oriented differently with respect to the dipole, which was always kept horizontal.

6. *The absolute measurement of the Pole brightness temperature.*—The same system was used as for the sky surveys. The beam was directed towards the North Celestial Pole for a few minutes. The aerial was then disconnected, a resistive load immersed in liquid nitrogen was substituted at point B, and the matching unit M_1 was adjusted to make the impedance of the substituted load equal to that of the comparison load. As in the sky surveys, a known amount of noise power was added to the aerial side of the switch to make the recorder deflection small while the Pole was being observed. The difference between the noise power available from the aerial and that from a resistive load at the temperature of liquid nitrogen was then known.

Observations were made between 1960 December and 1961 August, covering almost 24 hours of sidereal time. On several occasions, observations were made throughout the night to determine whether the noise power from the aerial stayed constant with time. Variations with a peak-to-peak amplitude of about 1 °K were indeed observed, the curve being roughly sinusoidal with maxima at 06^h and 18^h S.T. Calculations showed that the variations could be explained by the passage of the brighter parts of the sky, near the galactic plane, through the far-out H-plane side-lobes of the aerial and by the unequal widths of the main beam in the principal planes. The calculated peak-to-peak variation was 0·8 °K, which, incidentally, puts an upper limit on the proportion of linearly polarized radiation from the North Celestial Pole. This must, as observed with a 7°·5 beam, certainly be less than 0·5 °K. Since the Pole was used as a standard during the observations described in the previous section, a correction was applied for these variations in the noise power from the Pole.

The mean available noise power from the aerial corresponded to a temperature T_e of 36·0 °K with an estimated error of ±0·5 °K. The loss factor α of the feed and coaxial line to the point B was found, as described in Section 4 (ii), to be (2·2 ± 0·2) per cent. The temperature T_i for the Pole is obtained from the formula:

$$T_i = \frac{T_e - \alpha T_f}{1 - \alpha}$$

giving a value for T_i (Pole) of (30·3 ± 0·8) °K.

Using the experimental ground radiation curve of Fig. 4, with its zero level fixed as described in Section 4 (v), the temperature T_a' was found for the Pole.

TABLE I

Table of the temperatures T_a'

Dec. −20° R.A.	T_a'°K	Dec. −10° R.A.	T_a'°K	Dec. −5° R.A.	T_a'°K	Dec. 0° R.A.	T_a'°K	Dec. +5° R.A.	T_a'°K	Dec. +10° R.A.	T_a'°K	Dec. +15° R.A.	T_a'°K	Dec. +20° R.A.	T_a'°K
h m		h m				h m				h m				h m	
00 20	24·5	00 54	25·6			00 03	22·7			00 20	25·7			00 39	24·5
01 14	23·1	01 54	23·7			01 03	24·7			01 20	24·8			01 42	26·9
02 00	22·2	02 54	19·8			02 03	25·0			02 20	29·0			02 39	32·1
03 00	18·8	03 54	18·0			03 03	21·6			03 20	24·9			03 39	28·5
04 00	17·5	04 54	18·0			04 03	18·4			04 20	25·0			04 42	30·8
05 00	18·1	05 54	25·0			05 03	22·2			05 20	31·7			05 40	47·6
06 26	26·2	06 32	30·5			06 03	29·9			06 20	38·7			06 07	42·6
07 04	31·2	07 12	32·5			06 42	34·4			06 46	34·7			06 40	35·2
07 45	33·4	07 52	24·3			07 22	24·4			07 28	23·3			07 25	28·2
08 26	24·6	08 35	19·4			07 58	19·4			08 06	19·4			08 08	23·0
09 06	20·3	09 11	18·0			08 42	16·1			08 49	17·2			08 45	18·7
09 50	20·2	09 51	19·0			09 20	15·5			09 25	16·4			09 31	18·6
10 24	20·1	10 33	19·7			10 05	16·4			10 10	17·1			10 04	20·4
11 04	19·6	11 10	20·3	h m		10 40	17·7			10 47	17·9	h m		10 49	20·0
11 54	22·2	11 59	23·3	12 02	23·1	11 21	19·0	h m		11 27	19·9	11 26	20·3	11 29	20·5
12 28	25·0	12 33	26·1	12 39	26·5	12 07	22·5	12 12	20·3	12 17	22·8	11 58	21·1	12 08	20·5
13 14	27·8	13 20	25·2	13 25	23·7	12 42	27·6	12 48	26·6	12 51	27·6	12 18	24·6	12 28	20·5
13 48	28·3	13 54	26·7	13 41	24·8	13 30	23·3	13 35	23·8	13 37	27·0	12 54	26·7	13 00	21·7
14 10	32·7	14 34	30·0	14 40	28·7	14 04	24·7	14 07	24·2	14 11	27·4	13 38	29·8	13 44	29·5
15 04	36·2	15 05	33·8	15 17	30·5	14 43	28·1	14 48	29·2	14 53	32·2	14 09	32·1	14 15	34·5
16 08	39·2	15 54	35·9	16 01	32·9	15 21	28·9	15 26	33·2	15 29	37·9	14 55	36·0	15 00	35·9
16 21	44·0	16 26	40·3			15 36	29·3	16 08	39·0	16 14	44·8	15 24	39·4	15 45	41·9
16 40	50·2	16 46	41·5			16 03	32·1	16 34	42·5	16 39	47·7	15 45	43·7	16 21	42·7
17 06	64·4	17 10	52·0			16 33	39·7	16 58	49·2	17 01	55·1	16 16	47·6	16 50	41·3
17 28	94·0	17 36	74·7			16 52	43·5	17 24	55·9	17 25	60·4	16 43	49·4	17 11	40·5
17 56	215	18 04	130			17 21	51·0	17 48	64·0	17 53	58·8	17 24	50·1	17 33	40·7
18 21	188	18 25	208			17 44	66·0	18 16	76·9	18 21	67·4	17 41	49·4	18 01	45·4
18 48	81	18 52	113			18 09	100			18 43	102	18 12	54·0	18 30	54·0
19 12	50·0	19 17	69			18 31	157			19 06	135			18 51	60·7
19 57	32·9	19 39	47			18 58	150			19 33	80·6			19 15	77·0
20 24	29·8	20 10	36·6			19 21	83·7			19 58	46·6			19 39	72·4
21 14	28·0	20 54	31·9			19 46	49·9			20 23	37·8			20 03	48·9
22 14	24·0	21 54	28·6			20 13	39·0			21 20	28·8			20 36	36·4
23 14	24·9	22 54	24·3			21 03	31·0			22 20	26·8			21 38	32·4
		23 54	23·6			22 03	21·5			23 23	25·4			22 42	27·0
						23 03	23·1							23 41	23·9
θ=22°		θ=23°				θ=25°				θ=28°				θ=33°	

TABLE I—*continued*

Table of the temperatures T_a'

Dec. +25° R.A.	T_a'°K	Dec. +30° R.A.	T_a'°K	Dec. +40° R.A.	T_a'°K	Dec. +52° R.A.	T_a'°K	Dec. +60° R.A.	T_a'°K	Dec. +70° R.A.	T_a'°K	Dec. +80° R.A.	T_a'°K
		h m		h m		h m		h m		h m		h m	
		00 52	24·4	00 04	27·4	00 18	38·8	00 34	56·1	00 46	47·8	00 52	33·4
		01 52	22·7	01 04	27·7	01 18	38·1	01 34	54·7	01 46	46·1		
		02 53	29·7	02 04	32·4	02 18	40·0	02 34	58·5	02 46	42·6	02 52	31·9
		03 52	27·0	03 04	33·4	03 18	48·7	03 34	51·1	03 46	37·5		
		04 52	37·0	04 05	37·7	04 18	48·4	04 34	42·8	04 46	33·6	04 52	27·0
		05 52	35·6	05 05	41·1	05 18	39·1	05 34	35·7	05 46	31·0		
		06 17	32·2	05 45	31·8	05 56	34·3	06 10	33·4	06 46	27·6	06 52	23·8
		06 56	29·2	06 05	31·6	06 18	31·6	06 35	31·0	07 24	25·7		
		07 35	24·5	06 24	30·1	06 55	29·3	07 10	28·8	08 24	23·3	08 35	22·4
		08 19	20·4	07 05	27·4	07 56	24·9	08 10	26·6	09 24	23·0		
		08 57	17·5	07 45	24·5	08 55	21·7	09 10	24·4	10 25	23·6	10 35	22·2
		09 39	16·8	08 26	19·8	09 57	18·9	10 10	22·6	11 24	23·3		
		10 17	17·9	09 05	17·6	10 55	18·7	11 10	21·2	12 25	23·5	12 35	22·3
h m		11 00	18·6	09 48	16·5	11 55	20·5	12 12	21·8	13 25	22·9		
11 34	20·0	11 39	20·3	10 25	16·8	12 58	19·8	13 14	20·4	14 25	23·1	14 35	22·6
12 13	20·3	12 20	19·8	11 07	18·7	13 55	20·3	14 12	21·1	15 26	25·2		
12 32	20·1	12 38	19·8	11 46	19·5	14 58	20·4	15 10	22·7	16 25	26·5	16 35	23·6
12 59	19·6	13 12	20·0	12 25	19·6	16 05	24·2	16 15	25·5	17 28	27·6		
13 15	21·8	13 53	22·4	13 18	20·4	17 08	25·0	17 20	27·4	18 25	29·3	18 35	25·7
13 48	24·2	14 27	24·5	13 57	20·1	18 05	28·4	18 18	32·8	19 18	30·2		
14 21	27·5	15 11	25·9	14 29	20·9	19 03	35·9	19 15	34·3	20 25	32·9	20 35	28·8
15 05	32·5	15 44	27·8	15 09	23·4	20 05	46·5	20 14	34·8	20 46	33·8		
15 38	34·7	16 00	28·7	15 52	24·4	20 24	50·5	20 35	37·6	21 46	37·6		
16 18	35·4	16 25	29·5	16 31	25·2	21 17	65·2	21 34	48·5	22 46	42·6	22 52	31·1
		17 03	31·6	16 58	26·0	22 17	47·9	22 34	71·2	23 46	46·2		
		17 36	32·6	17 57	28·8	23 20	38·4	23 35	98·0				
		18 05	36·9	18 55	33·5								
		18 36	42·3	19 21	42·2								
		18 58	45·0	19 57	123								
		19 21	50·7	20 20	109								
		19 47	67·9	21 00	64·1								
		20 11	65·9	22 03	36·1								
		20 52	46·4	23 07	29·0								
		21 52	31·2										
		22 52	24·7										
		23 53	27·0										
		$\theta=40°$		$\theta=52°$		$\theta=73°$		$\theta=85°$		$\theta=62°$		$\theta=37°$	

ote: θ is the angle between the meridian and the H plane for the region enclosed by the lines. Outside this region θ is zero.

This was $(25{\cdot}0 \pm 2{\cdot}0)$ °K, where the error includes the estimated uncertainty in the corrections for T_g and T_0. This value of T_a' (Pole) is an average over 24 hours of sidereal time and includes the average contributions of side-lobes outside the main beam during this period. The corresponding T_a (Pole) is 24·3 °K; the calculated mean $T_s = 4{\cdot}0$ °K so that T_m (Pole) $= 20{\cdot}3$ °K and T_b (Pole) $=$ $(23{\cdot}9 \pm 2{\cdot}0)$ °K.

7. *The results.*—The measurements are presented in Table I as the temperatures T_a' of a loss-free aerial from which the contributions given by Fig. 4 (solid curve) have been subtracted. No corrections for power received from regions of the sky outside the main beam have been made in this table. The region of sky between α 16^h and 20^h was not observed at transit; the angle between the H-plane and the meridian, normally zero, is given for each declination in this region.

Although the number of points observed was insufficient to acquire all the information in principle attainable with this aerial, contour maps have been made with the aid of this grid of values by drawing smooth curves through the points. These contour maps, plotted in celestial and galactic coordinates, are given in Figs. 5, 6, 7 and 8.

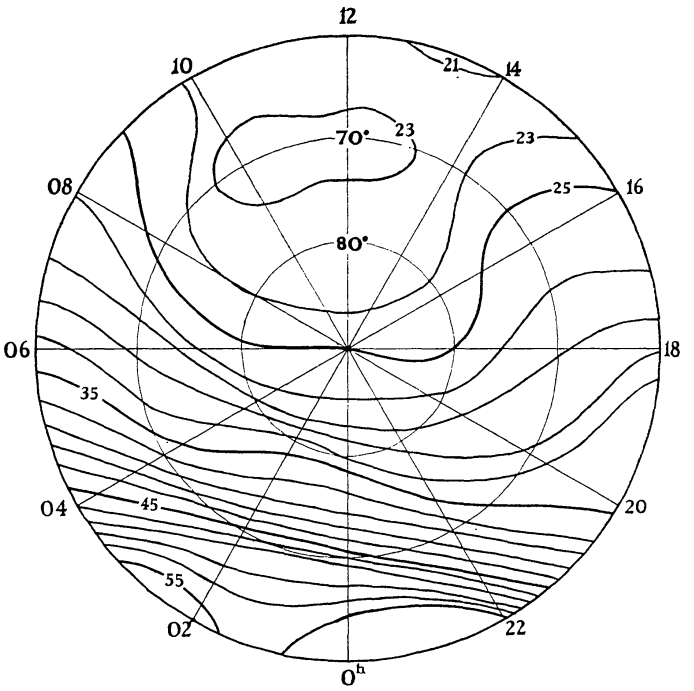

FIG. 5.—*Contours in celestial coordinates of T_a', defined in Section 4(i). Over most of the sky T_a' is nearly equal to the brightness temperature.*

In Table II are presented the corrections required to obtain T_m, the main beam contribution. Two numbers are given at each right ascension and declination. The first is the correction which gives T_a from T_a' by allowing for the error in the solid curve of Fig. 4. The second is the sky contribution in side-lobes T_s. Subtracting both these numbers from T_a' gives T_m at the appropriate point. The beam temperature T_b is then found from the relationship:

$$T_b = T_m / 0{\cdot}85$$

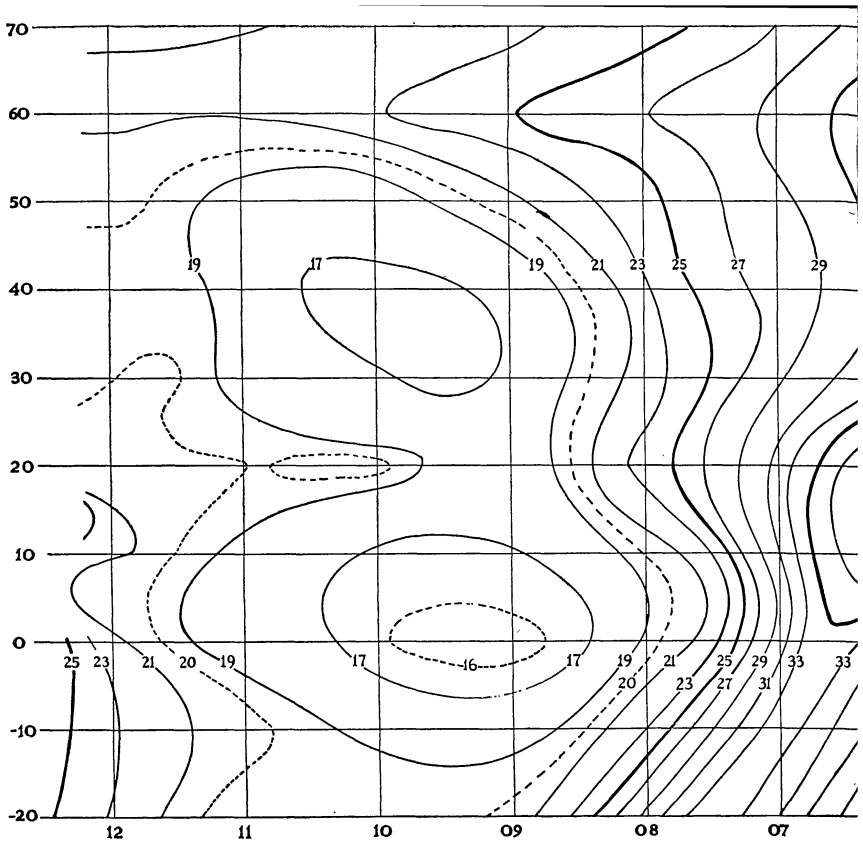

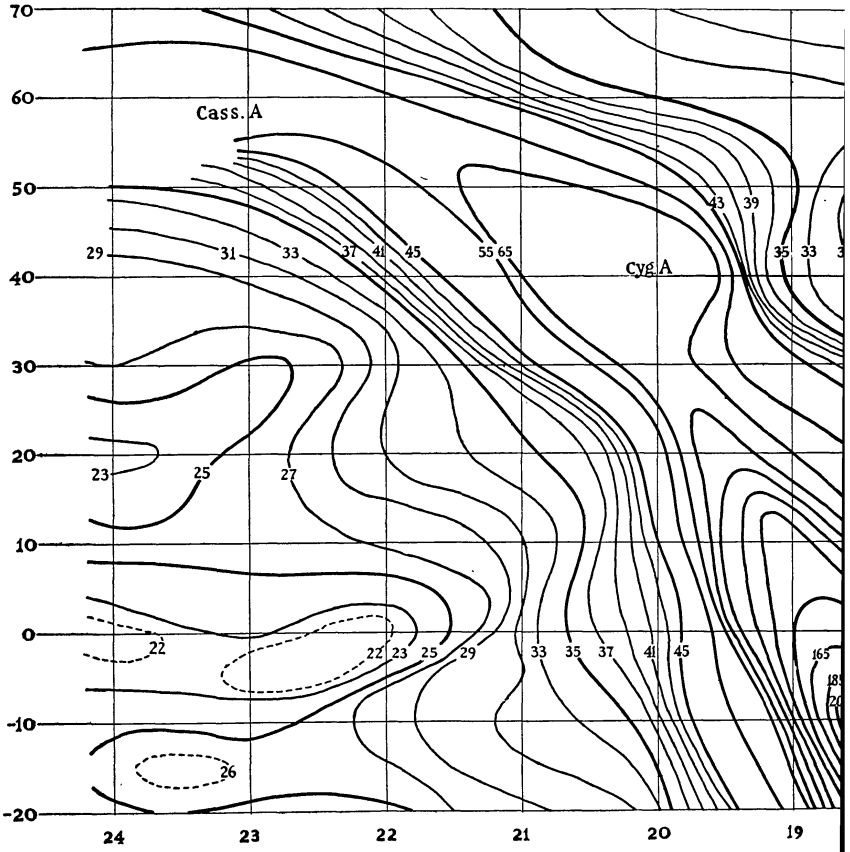

Contours of the t

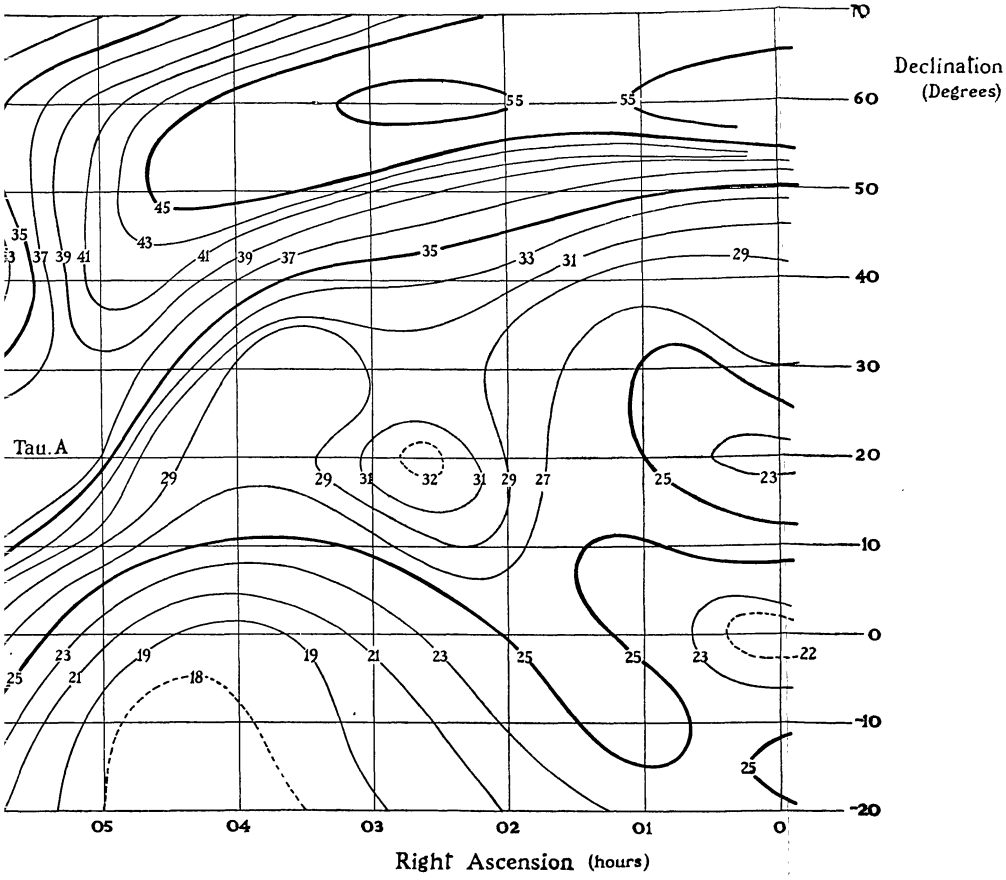

FIG. 6

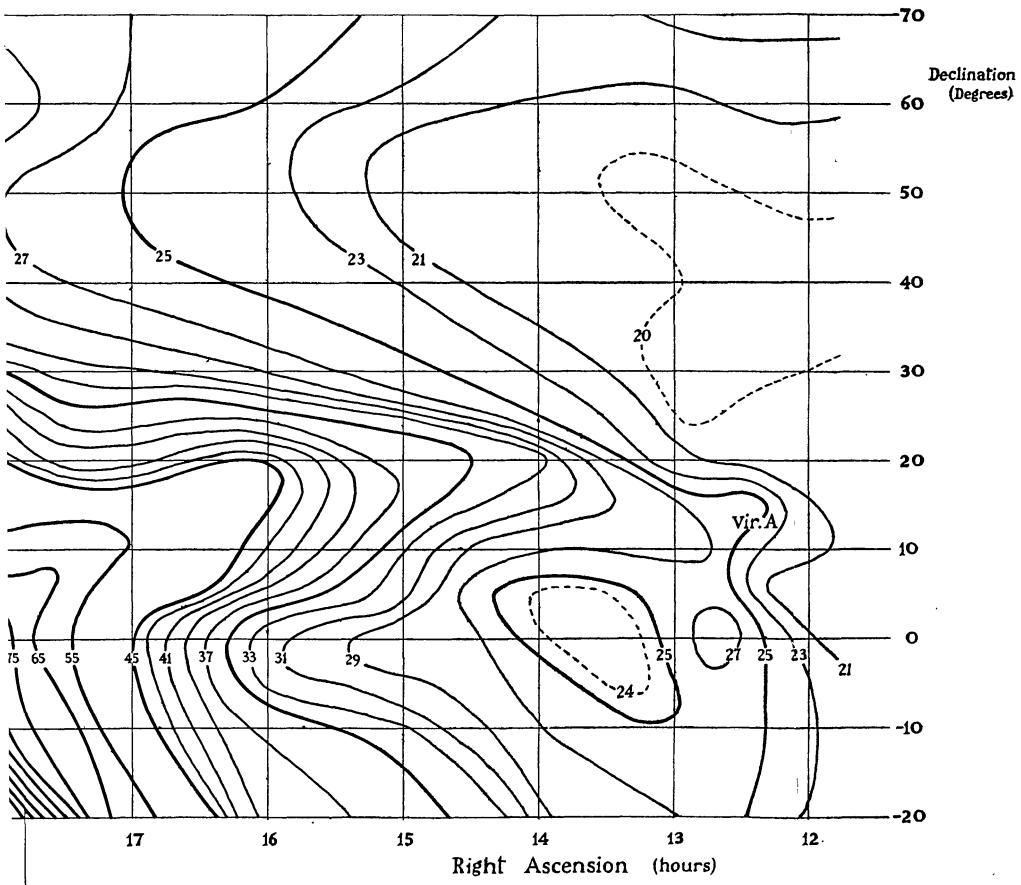

FIG. 7

es T_b' in celestial coordinates.

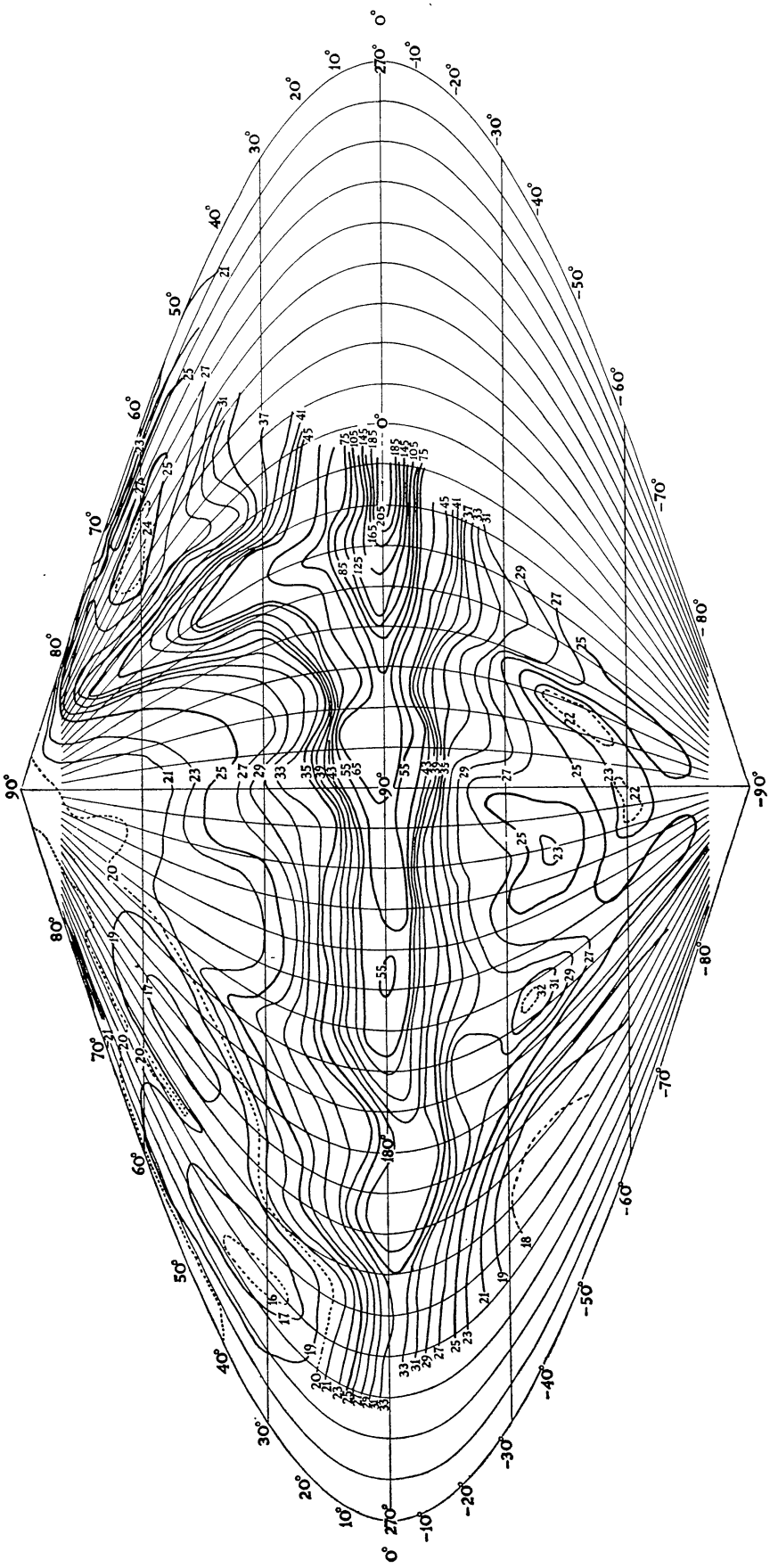

FIG. 8.—*Contours of the temperatures T_a' in new galactic coordinates.*

TABLE II

δ \ α(h)	0	2	4	6	8	10	12	14	16	18	20	22
70°	0·4	0·4	0·4	0·4	0·4	0·4	0·4	0·4	0·4	0·6	0·4	0·4
	4·4	4·3	4·2	4·1	4·0	3·8	3·7	4·0	4·6	4·6	5·2	4·6
52°	0·0	0·0	0·0	0·0	0·0	0·0	0·0	0·0	0·0	0·5	0·0	0·0
	4·8	4·4	4·6	4·4	4·0	3·7	3·8	4·2	4·9	5·1	6·1	4·8
30°	0·5	0·5	0·5	0·5	0·5	0·5	0·5	0·5	0·5	0·6	0·5	0·5
	4·2	4·1	4·1	3·9	3·7	3·2	3·5	3·8	4·8	5·6	5·9	5·0
10°	0·7	0·7	0·7	0·7	0·7	0·7	0·7	0·7	0·7	0·7	0·7	0·7
	3·6	3·6	3·6	3·4	3·1	2·9	2·8	3·3	4·7	5·6	5·6	4·1
−10°	0·9	0·9	0·9	0·9	0·9	0·9	0·9	0·9	0·9	1·0	0·9	0·9
	3·2	3·1	3·0	2·8	2·6	2·5	2·4	3·3	4·4	5·6	5·6	3·8

The region enclosed by the lines is observed off transit. The numbers are calculated for the different orientations of the beam in this region.

The errors in the measurements are as follows:

Random errors

(i) The scatter of measurements made on successive nights; the average error was about ±0·5 °K.

(ii) The error in the calibration of the noise source, which was about ±2 per cent, that is, an error of ±0·3 °K in the least bright regions of the sky and ±4 °K in the brightest regions. Since the calibration was the same for all measurements, the fractional error in the aerial temperature differences is a constant over the sky.

Systematic errors

(i) Any error in the measured pole temperature and the corrections applied to it. This gives a constant error of ±2·0 °K over the whole sky.

(ii) Any error in the subtraction of ground radiation for points not at the zenith. The largest correction was 11 °K, for declination −20°, and the largest error in such a correction should have been less than ±0·5 °K.

(iii) Since only one component of polarization was measured, the presence of a linearly polarized component in the radiation (**11**) would give rise to errors. Measurements made by the authors and Mr R. Wielebinski (**12**) indicate that over most of the sky such a component contributes less than 1 °K.

The average error in the brightness temperature difference between any two points observed is thus ±0·8 °K and the error in the absolute temperature at an average point is about ±2·2 °K.

In a comparison with another survey, the error made in correcting for the effect of side-lobes is of interest. If the power in the main beam is in the range 81 per cent to 89 per cent, the error in T_b is ±0·3 °K for $T_a = 30$ °K up to ±3 °K for $T_a = 100$ °K. Any errors in the measurement of the reception pattern are estimated to lie within this range.

Acknowledgments.—Our grateful acknowledgments are due to Professor Martin Ryle for some valuable discussions and to A. Rogers and R. Wielebinski for assistance with the observing programme.

Mullard Radio Astronomy Observatory,
Cavendish Laboratory,
Cambridge:
1961 *December*.

References

(1) A. J. Turtle and J. E. Baldwin, to be published.
(2) S. Kenderdine and J. E. Baldwin, to be published.
(3) A. J. Turtle *et al.*, to be published.
(4) C. Seeger, F. L. H. M. Stumpers and N. van Hurck, *Phil. Tech. Rev.*, **21**, No. 11, 317, 1959.
(5) M. I. Large, D. S. Mathewson, and C. G. T. Haslam, M.N., **123**, 112, 1961.
(6) R. H. Dicke, *Rev. Sci. Instr.*, **17**, 268, 1946.
(7) F. G. Smith, *Proc. I.E.E.*, **108B**, No. 38, 201, 1961.
(8) G. D. Monteath, *Proc. I.E.E.*, **102B**, 383, 1955.
(9) D. C. Hogg, *J. Appl. Phys.*, **30**, 1417, 1959.
(10) S. Kenderdine *et al.*, to be published.
(11) H. C. van de Hulst, *Konink. Ned. Ak. van Wetenschappen*, **70**, No. 2, 1961.
(12) R. Wielebinski, J. R. Shakeshaft and I. Pauliny-Toth, to be published.